



OPEN ACCESS

EDITED BY
Chunquan Yu,
Southern University of Science and
Technology, China

REVIEWED BY
Yosuke Aoki,
The University of Tokyo, Japan
Mingjie Liu,
Southwest Petroleum University, China
Meng Li,
SINOPEC Petroleum Exploration and
Production Research Institute, China

*CORRESPONDENCE
Zhong Li,
✉ lizhong@mail.iggcas.ac.cn

SPECIALTY SECTION

This article was submitted to Structural
Geology and Tectonics,
a section of the journal
Frontiers in Earth Science

RECEIVED 08 October 2022
ACCEPTED 18 January 2023
PUBLISHED 02 February 2023

CITATION
Liang S, Li Z, Zhang W and Gao Y (2023),
The characteristics of strike-slip faults and
their control on hydrocarbon distribution
in deep carbonate reservoirs of the central
Sichuan Basin.
Front. Earth Sci. 11:1064835.
doi: 10.3389/feart.2023.1064835

COPYRIGHT
© 2023 Liang, Li, Zhang and Gao. This is an
open-access article distributed under the
terms of the [Creative Commons
Attribution License \(CC BY\)](#). The use,
distribution or reproduction in other
forums is permitted, provided the original
author(s) and the copyright owner(s) are
credited and that the original publication in
this journal is cited, in accordance with
accepted academic practice. No use,
distribution or reproduction is permitted
which does not comply with these terms.

The characteristics of strike-slip faults and their control on hydrocarbon distribution in deep carbonate reservoirs of the central Sichuan Basin

Shangzi Liang^{1,2}, Zhong Li^{1,2*}, Wang Zhang¹ and Yang Gao³

¹State Key Laboratory of Lithospheric Evolution, Institute of Geology and Geophysics, Chinese Academy of Sciences, Beijing, China, ²College of Earth and Planetary Sciences, University of Chinese Academy of Sciences, Beijing, China, ³Oil and Gas Resources Strategic Research Center of the Ministry of Natural Resources, Beijing, China

The past decade has witnessed a breakthrough in the gas exploration of deep marine carbonates of the central Sichuan Basin. Deep faults research has also attracted increasing attention, as faulting plays an important role in reservoir control. Previous studies have suggested a developed series of high-angle strike-slip fault systems in the central Sichuan Basin, but correlated exploration activities are limited, as distribution rules and dynamic mechanisms remain unclear. In this study, the spectral decomposition coherence method was used to describe the geometric and kinematic characteristics of these strike-slip faults. Using a comprehensive analysis technique to assess the strike-slip fault tectonic activity history, the formation and evolution processes of strike-slip faults and their control on hydrocarbon distribution were examined. The results showed that the deep strike-slip fault system, mostly distributed in the Dengying Formation, can be divided into four stages, three levels, and three groups of orientation, which controlled the structural framework and shape of the central Sichuan area, as well as the zoning from north to south, and blocking from west to east. The faults showed features of layered deformation and staged evolution in the vertical direction. The segmentation of strike-slip faults strongly controls the quality of fractured vuggy reservoirs. Reservoirs of the hard-linked zone of the strike-slip fault are the most developed, followed by those of soft-linked segments, with translational sections of the strike-slip fault being relatively undeveloped. Strike-slip faults are important hydrocarbon migration paths, and their multistage activities have different controlling effects on hydrocarbon accumulation.

KEYWORDS

deep strike-slip faults, deep carbonate reservoir, hydrocarbon distribution, Central Sichuan Uplift, Sichuan Basin

1 Introduction

Global carbonate formations are rich in hydrocarbon resources, and will likely be the most important area for future oil and gas exploration and development. Dedicated research in China has led to globally recognized discoveries in the marine carbonate formations of the Tarim, Sichuan, and Ordos Basins. Recently, carbonate oil and gas exploration has gradually moved into deep (burial depth >4500 m) and ultra-deep (>6,000 m) carbonates with increasing progress in exploration technology, resulting in new discoveries of various oil and gas resources (Liu et al., 2009; Li et al., 2020; He et al., 2021; Liu et al., 2010). Most marine carbonates in China are formed in the lower part of the superimposed basin, characterized by

deep burial and ancient origin, and have undergone complex diagenesis along with multi-phase tectonic movements during its geological history. Faults and concomitant joints accompanying the multi-stage tectonic evolution could both act as passageways for oil, gas, hydrothermal, and volcanic fluids, as well as playing an important role in later reservoir transformations and hydrocarbon accumulation.

Since 2006, with the discovery of the Anyue gas field, the Gao Shi 1 and Moxi 8 wells in the central Sichuan area have been drilled and tested to obtain a high-yielding industrial gas flow from the Sinian-Cambrian dolomite reservoir, confirming the huge exploration potential of deeper layers in central Sichuan. Previous studies in this region have focused on tectonic evolution, sedimentary facies distribution, and hydrocarbon migration and accumulation. Influenced by the traditional concept of the stable central Sichuan block, previous studies on the deep fault system of the central Sichuan Basin remain incomplete. Currently, there is consensus on the development of deep strike-slip faults in the central area of the Sichuan Basin, but there are still controversies regarding the distribution pattern, nature, and formation period of said faults. Yin et al. (2013) suggested that deep fault systems formed during the Caledonian tectonic period, and experienced multiple stages of strike-slip fault activity in the Hercynian, Indosinian, Yanshan, and Himalayan epochs. According to Li (2017), strike-slip faults existed in two phases of development, at the end of the Sinian and the end of the Early Cambrian. However, Ma et al. (2018) suggested that the strike-slip faults in the Central Sichuan Uplift experienced two stages of activity: Early Caledonian and Late Hercynian. Su et al. (2020) proposed that the principal fault activity occurred during Himalayan formation, revealed by shallow high-steep faults cutting through the Jurassic strata in central Sichuan, and the deep strike-slip faults are in the same fault system. In the present study, the geometrical and kinematic characteristics of strike-slip faults are described based on filtering and spectrum decomposition techniques. The relationships between strike-slip faults, reservoir modification, and oil-gas accumulation are also discussed. This study has great scientific significance for finding out the development characteristics of the strike-slip faults and their control on hydrocarbon accumulation in stable parts of cratonic basins, including the Ordovician strike-slip faults in Tazhong and Tabei areas of Tarim Basin, and the Triassic Yanchang Formation strike-slip faults in Ordos Basin.

2 Geological setting

2.1 Regional geology

The Sichuan Basin covers an area of approximately $1.8\text{--}3.0 \times 10^5 \text{ km}^2$ in western China. It is a superimposed basin that developed on the Neoproterozoic crystalline basement of the Yangtze Craton, limited by the Animaqing-Mianlue suture in the north, the Longmenshan tectonic belt in the west, the Ganzilitang suture in the southwest, and the east Sichuan folded belt in the east (Figure 1A; Wei et al., 2019). According to the oil and gas resource evaluation from the China National Petroleum Corporation, the total geological reserves of natural gas in the Sichuan Basin are $3.818 \times 10^{13} \text{ m}^3$, and the total cumulative conventional gas production is $\sim 5.998 \times 10^{11} \text{ m}^3$, making it the largest natural gas producing area in China. Based on the

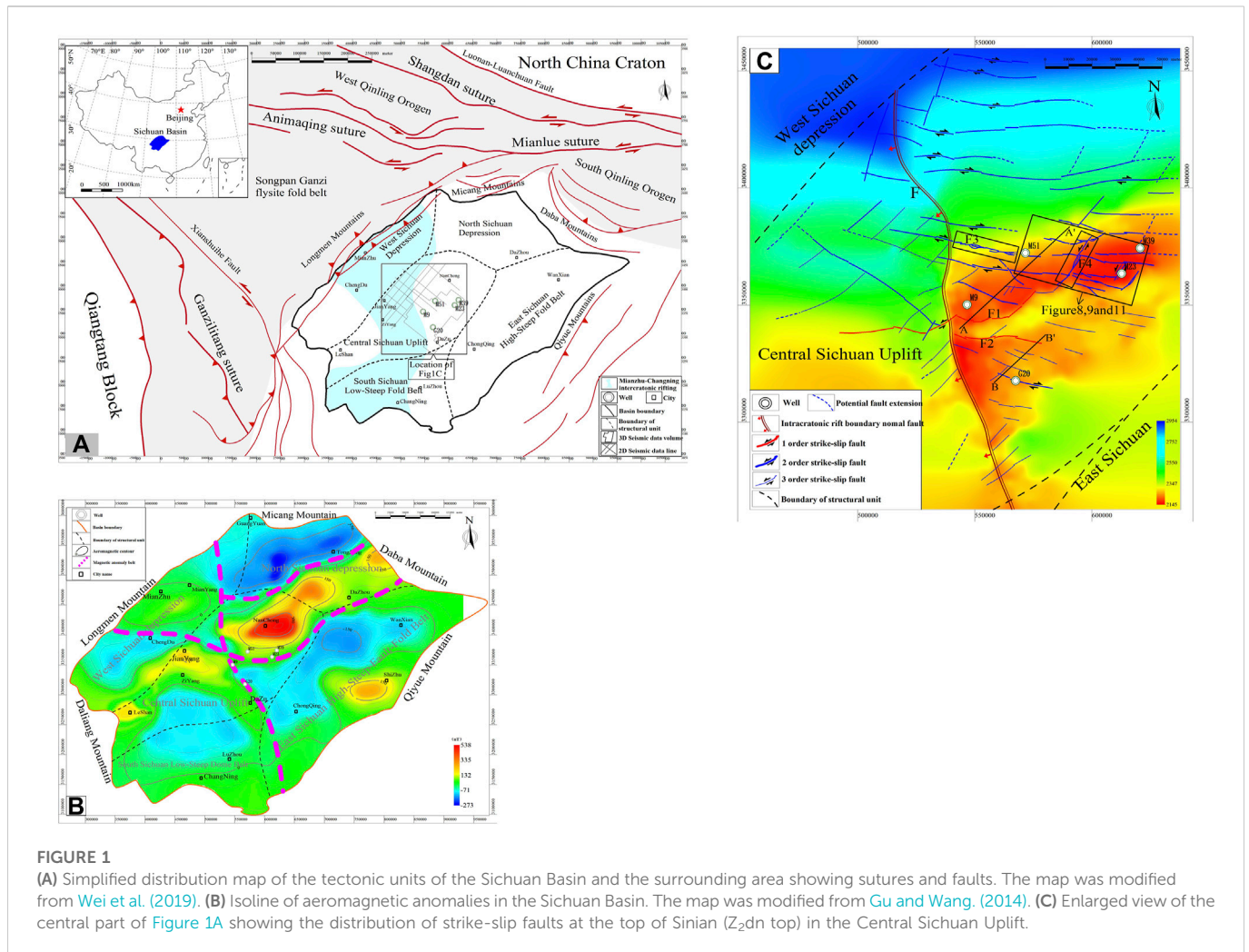
morphological and geometrical characteristics of the present-day top of the Sinian, the Sichuan Basin is divided into five primary tectonic units: the Central Sichuan Uplift, West Sichuan Depression, North Sichuan Depression, East Sichuan High-Steep Fold Belt, and South Sichuan low-steep fold belt (Figure 1A). The Central Sichuan Uplift is located in the central part of the Sichuan Basin, which is characterized by a giant long-axis anticlinal structure spreading to the northeast (Figure 1C), and the structure was fixed in the Yanshan-Himalayan period.

The study area is located in the Central Sichuan Uplift and covers an area of $24,500 \text{ km}^2$. Structural research shows that it contains the GaoShiti-Moxi paleo-uplift, and the Mianzhu-Changning Cratonic internal rifting to the west. The western boundary of the GaoShiti-Moxi paleo-uplift is the north-south striking synsedimentary normal fault F dipping to the west (Figure 1C). There is no other obvious tectonic boundary to the north, east or south, indicating a transitional relationship. The strike-slip fault system (Yin et al., 2013; Ma et al., 2018; Su et al., 2020; Liang and Li, 2022), a product of multiple tectonic movements on the periphery basin, was developed in the deep part of the study area.

Marine carbonates are mainly developed in the Sinian to Middle Triassic, and the Upper Triassic-Quaternary are terrestrial deposits (Figure 2). Taking into account the lithological differences between Sinian-Permian, the lower Triassic-middle Triassic, and upper Triassic, and the unconformities, the central Sichuan area was divided into a lower structural sequence (Sinian-Permian), a middle structural sequence (Lower Triassic-Middle Triassic), and an upper structural sequence (Upper Triassic and its overlying strata). The strike-slip faults in the study area are mainly distributed in the lower structural sequence. The majority of the exploratory wells in the central Sichuan area did not penetrate the Sinian. Industrial hydrocarbon flows revealed by the drilled wells are related to marine carbonates, including the Sinian, Cambrian, Carboniferous, Qixia-Maokou, Changxing, Feixianguan, Jialingjiang, and Leikoupo formations. The Sinian contains two sets of high-quality reservoirs, namely the second and fourth members of the Dengying Formation. Their lithologies are primarily algal-clotted dolomite, algal-stromatolitic dolomite, algal dolarenites, and oncolite, with a wide horizontal distribution stacked vertically against each other. The reservoir in the fourth member of the Dengying Formation has experienced strong karstification of weathering crust, leading to increased reservoir porosity and forming a fracture-void system due to multiple stages of dissolution and tectonic movement. The stratigraphic contacts between the fourth member of the Dengying Formation and overlying Lower Cambrian Qingzhusi Formation are unconformities. Karstification of the reservoir took place near the unconformity of the Dengying Formation, forming the largest deep marine carbonate gas field in China.

2.2 Tectonic evolution of the region

Basement activity and pre-existing basement fractures in the Sichuan Basin are stress concentration zones (Nemcok et al., 2005;



[Tong et al., 2010](#)), which not only control the development and evolution of sedimentary cover in the basin, but also are important factors triggering the development of faults within the sedimentary cover. Previous studies have shown that the central area of the Sichuan Basin is to the northeast, near the west–east magnetic anomaly belt ([Figure 1B](#)), whereas a negative magnetic anomaly belt developed between the two positive magnetic anomaly belts in the northeast and southwest. A negative magnetic anomaly belt developed between the positive magnetic anomalies in Jianyang and Dazu, and weak positive magnetic anomalies developed to the south of the strong positive magnetic anomalies in Nanchong; therefore, the basement of the central area of the Sichuan Basin is not a unified block, but rather comprises several large tectonic weak zones based on aeromagnetic anomalies ([Gu and Wang, 2014](#)). As weak tectonic zones, the basement faults are prone to be active under the regional stress field, which may form the basis of the development of the west-east and north-east strike-slip faults in the central area of the Sichuan Basin.

The fault evolution of the Sichuan Basin is closely related to basin basement activity, and the remote effects are generated by the convergence or divergence of the surrounding plates. From the Late Neoproterozoic to the Cambrian, the paleo-Qinling oceanic crust to the north of the Yangtze Plate was subducted below the Yangtze plate by the influence of the breakup of Rodinia. With an

increasing dip in the subduction zone, the dynamic mechanism of the South Qinling Plate changed from a subduction–convergence mechanism to one of retreat–extension ([Zhu et al., 2014; 2015; Hu et al., 2015; Xiang et al., 2015; Wang et al., 2017; Zhang et al., 2018](#)), forming an interior rifting of the Yangtze Plate due to the tensional setting ([Niu et al., 2003; Stein and Stein, 2013](#)). Simultaneously, the western margin of the Yangtze Plate converged to the northern margin of East Gondwana by subduction ([Moghadam et al., 2013; Chen et al., 2018](#)), resulting in a transtensional setting within the Yangtze Plate due to slab pull. Based on the above two factors, the western margin of the Yangtze plate developed the north-south Mianzhu-Changning intracratonic rift ([Zhu et al., 2007; Jiang et al., 2011; Liu et al., 2013; Li et al., 2019](#)). The central area of the Sichuan Basin, located at the western margin of the Yangtze plate is influenced by the Mianzhu-Changning intracratonic rift, and includes a series of synsedimentary faults ([Figure 3B](#)).

The Yangtze plate drifted slowly northwards in the transtensional setting, reaching a maximum drift rate and rotating anticlockwise during the Ordovician, due to strong tectonic activity ([Figure 3A; Feng et al., 2011; Hou et al., 2014](#)). Owing to slab retreat and mantle uplift, the margin and interior of the Yangtze Plate have both extensional and uplift dynamic mechanisms ([Figure 3C](#)). Based on the pre-existing tectonic weak zone, the central Sichuan area is subject to oblique transtension near west-east and north-east strike-slip faults.

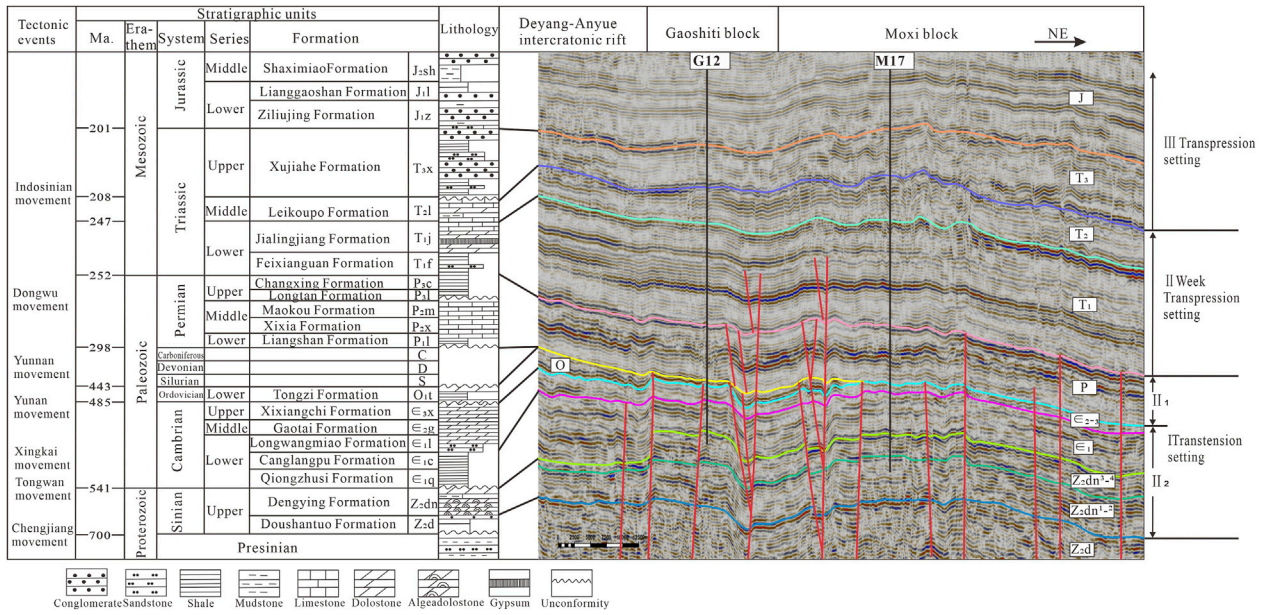


FIGURE 2 Comprehensive tectonostratigraphic column of Central Sichuan Uplift, Sichuan Basin.

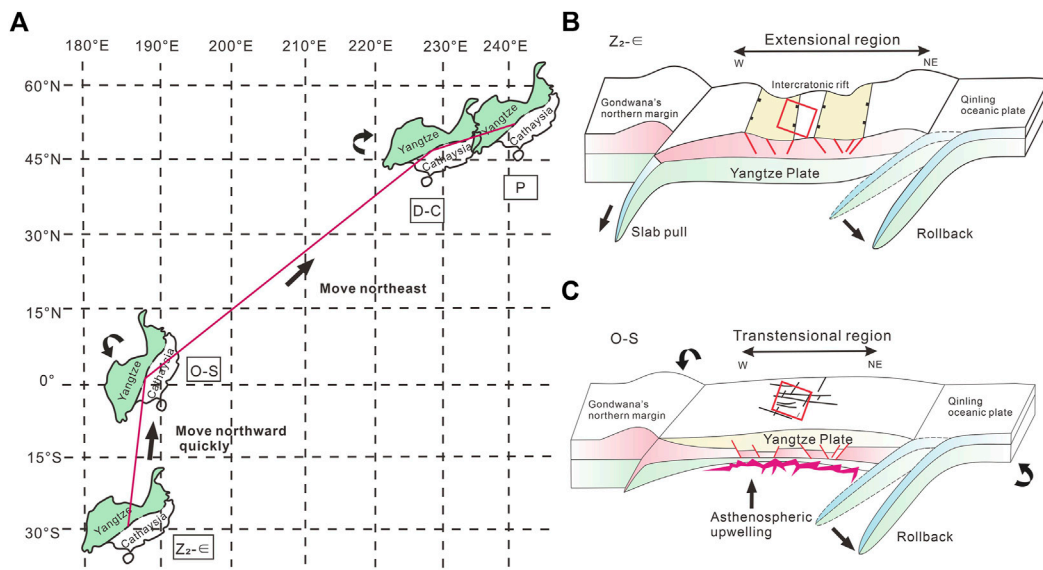


FIGURE 3 (A) The displacement and rotation of the Yangtze Plate from the Sinian to Permian based on palaeomagnetic data by Luo et al. (2004); Feng et al. (2011) and Hou et al. (2014). (B) Tectonic evolution of the central area of Sichuan Basin with synsedimentary faults, serving as the east boundary of the Mianzhu-Changning intercrateric rift. (C) Tectonic evolution of the central area of Sichuan Basin with strike-slip faults.

Under the influence of the hot doming of mantle uplift, and the opening of the ancient Tethys Ocean, the Sichuan Basin started to rift from the Middle Devonian within the Yangtze Plate, and the Emei basalt eruption reached its maximum in the Late Permian. At the end of the Early Permian, the subduction of the Qiangtang terrain resulted in southwest-

northeast transpressional stress, causing north-west rifting of the Yangtze plate, and accelerating the up-arching of the deep “Emei Mantle Column,” resulting in rapid eastward movement (Figure 3A; Luo et al., 2004). Here, the coinciding tectonic activity was the strongest. The main faults in the central Sichuan area have undergone inherited development.

Beginning in the Late Triassic, the Upper Yangtze region, including the Sichuan Basin, was mainly influenced by peripheral compressional stress, ending the evolution of the intracratonic rift-style basin, and leading to the development of a series of foreland basins. The strike-slip faults of the central Sichuan area were adjusted and modified in a transpressional regime because of the collocation of the surrounding plates.

3 Data and methods

3.1 Database

Core data, well data, imaging logs, and 2D and 3D seismic data were used in the present study. Core samples were obtained from ten exploratory wells of the fourth member of the Dengying Formation, whereas well data, including conventional electrical log curves and lithological logs, were collected from 80 exploratory wells in the central Sichuan area. The post-stack time migration 3D seismic data covered an area of 8,000 km² (Figure 1A), with a cell size of 20 × 20 m, a sampling interval of 2 m, an effective frequency band range of 12–49 Hz, and a deep dominant frequency of 30 Hz (Figure 12). Eleven (11) two-dimensional seismic lines totaled 1,300 km (Figure 1A).

3.2 Methods

As the depth increases, the resolution and dominant frequency of seismic data will decrease. The Strike-slip fault has the characteristics of small displacements and is difficult to identify. To enhance the sensitivity of different scales of faults from seismic data, this study used an improved coherence technique based on spectral decomposition to describe medium-small scale faults. The original full spectral-band post-stack time migration seismic data were decomposed into 15, 25, 35, and 45 Hz frequency-divided data. The results showed that the seismic profiles from the 35 Hz frequency-split data had higher resolution and clearer breakpoints; thus, the 35 Hz frequency band was identified as the dominant frequency for deep fault spectrum decomposition processing in this area. The edge-preserving filtering method (An et al., 2021) can effectively protect discontinuous boundary information, improve the signal-to-noise ratio, and enhance the continuity of seismic events. After spectral decomposition and filtering, the seismic data were used as a carrier to extract coherent attributes, curvature, and ant-tracking data along the target layer to characterize the faults and fractures (Ma et al., 2020).

When a significant acoustic impedance difference exists between the reservoir and non-reservoir rocks, the reservoir can be predicted using conventional post-stack seismic attributes. The porosity of the carbonate rocks of the Sinian Dengying Formation calculated from its logging curve decreased with increasing acoustic impedance, revealing a negative correlation; therefore, the porosity ranges can be used to define the acoustic impedance values of the reservoir and non-reservoir rocks. Compared with the post-stack seismic amplitude method, the principal component analysis (PCA) of the frequency-decomposed amplitude can significantly improve reservoir thickness prediction. The post-stack seismic data were subdivided into low-, mid-, and high-frequency panels, extending the amplitude tuning range, and improving the amplitude-thickness linear relationship

(Zeng, 2017). The frequency-decomposed amplitude attributes extracted from the low-, mid-, and high-frequency panels were transformed into principal components, extracting most of the seismic attribute information (Chopra and Marfurt, 2007). The relationship between the frequency-decomposed amplitude principal components and reservoir thickness at the well site was fitted and calculated. In this study, 15 wells were used for the fitting calculation, and the correlation coefficient (R^2) between the predicted and actual values was 0.78. The predicted results for the other five blind-testing wells fell within the predicted trend, indicating that the seismic prediction results were credible.

4 Results

4.1 Strike-slip fault characteristics from seismic data

Based on the refined interpretation of the processed seismic data, three groups of deep strike-slip faults trending north-east, north-west, and west-east were identified in the study area, and the fault structure styles in both section and planar distribution patterns were clarified. At the eastern boundary of the Deyang-Anyue intracratonic rift, the nearly north-south trending syndimentary fault F separated the western and eastern fields of the study area (Figure 1C). The region in the west primarily shows north-west and north-east trending strike-slip faults, whereas the eastern field is developed with north-east, north-west, and nearly west-east trending strike-slip faults. Fault F1 divided the study area into the northern Moxi structure and the southern Gaoshiti structure. Compared to the Gaoshiti structure, the Moxi structure shows more faults and stronger fault activity. In the Moxi structure and its northern slope, the strike-slip faults exhibit north-west, north-east, and nearly west-east trends that are roughly perpendicular to the central area of the Sichuan Basin. The entire major fault consists of several segmental faults with different dips and throws, and the planar structural characteristics vary along the strike. Together, with the coherent attributes extracted from the seismic data processed by spectrum decomposition and filtering (Figure 4), and fault characterization by the ant-tracking technique, the planar distribution pattern of strike-slip faults exhibits echelons, oblique intersections, and arc shapes. The Gaoshiti structure and its southern slope mainly developed northwest trending faults, and generally, the single north-west trending fault exhibited a short extension distance and vertically ended at the bottom of the Permian. The fine coherence map shows that secondary faults within north-west trending faults are distributed in an en-echelon arrangement, further confirming that the north-west trending faults are dextral strike-slip faults. In general, the number of faults in the southern belt (Gaoshiti structure and its southern slope) is markedly less than in the northern belt (Moxi structure and its northern slope). The structural pattern of the strike-slip fault assemblage is classified into three levels according to the activity periods, extension length, and horizon cut-through by fault (Figure 1C). For example, fault F1 serves as the boundary of the Moxi structure: it penetrates the basement, terminates upward in the Triassic, shows a large fault throw, a long distance of planar

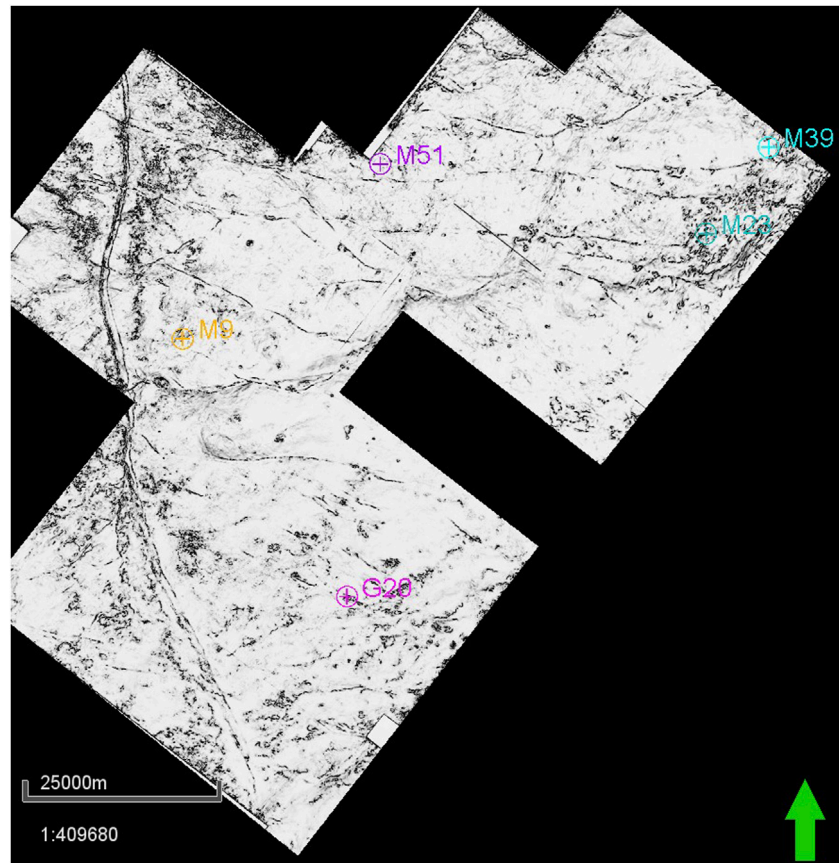


FIGURE 4

Fine coherent map of the top surface of the Dengying Formation in the 3D seismic area. See [Figure 1A](#) for location.

extension, a significant horizontal slip displacement, and multi-stage activity. It is therefore considered a first-grade fault. Second-grade faults present a smaller scale than the first-grade, generally extend across the Sinian, and end during the Cambrian, which controls the development of secondary fault blocks.

The seismic sections displayed in [Figure 5](#) represent typical images of deep strike-slip faults mapped to 3D seismic volumes ([Figures 1C, 4](#)). These faults are characterized by steeply dipping, half-flower positive flower, and negative flower structures in the study area. Owing to the superposition of multistage structural deformations, multiple flower structures develop in local areas, forming a superposition of these structures on the seismic profile. The steeply dipping fault is characterized by the development of a single main fault without branch faults. Its fracture zone is narrow and steep, with small fault throws, most of which are transtensional. As a special vertical configuration style of the main and branch faults, the flower structure is one of the typical signs for the identification of strike-slip faults. The strike-slip faults in the central Sichuan area show a negative flower structure feature during the Sinian-Ordovician, similarly indicating that the nature of the faults is transtensional. Owing to the lithological differences between the Permian and its underlying strata, the influence of large unconformities formed by the superposition of multiple unconformities between the Permian strata and its underlying strata, as well as the structural deformation of strike-slip faults are characterized by layered deformation in the longitudinal

fault systems in the study area. The faults in the Permian are in the form of small grabens or horsts, which partly converge downward in the boundary of the lower flower structure, and partly in the middle main sliding surface, revealing that the fault development position and strength in the Permian are closely related to the lower strike-slip fault and later fault activity. Some of the strike-slip faults terminate upward in the Triassic, and develop a positive flower structure, forming a raised stratigraphic deformation along the faults, or exhibiting the characteristics of small horsts.

4.2 Linkage and segmentation of strike-slip faults

Previous studies have suggested that the growth of large faults does not evolve from an infinite extension of a secondary fault, but rather from a series of secondary splays (segments) that rupture, spread, grow, interact, and link in a similar orientation ([Kim and Sanderson, 2005](#); [Aydin and Berryman, 2010](#)). According to the stress and strain in the overlapping and tip zones of the fault, the fault formation process is characterized by segmentation ([Choi et al., 2016](#); [Khalil and Mccday, 2016](#)). Segments are isolated from each other at intervals of hundreds of meters, showing disconnection and no interaction, and can be considered as isolated fault segments. Soft-linked segments are generally

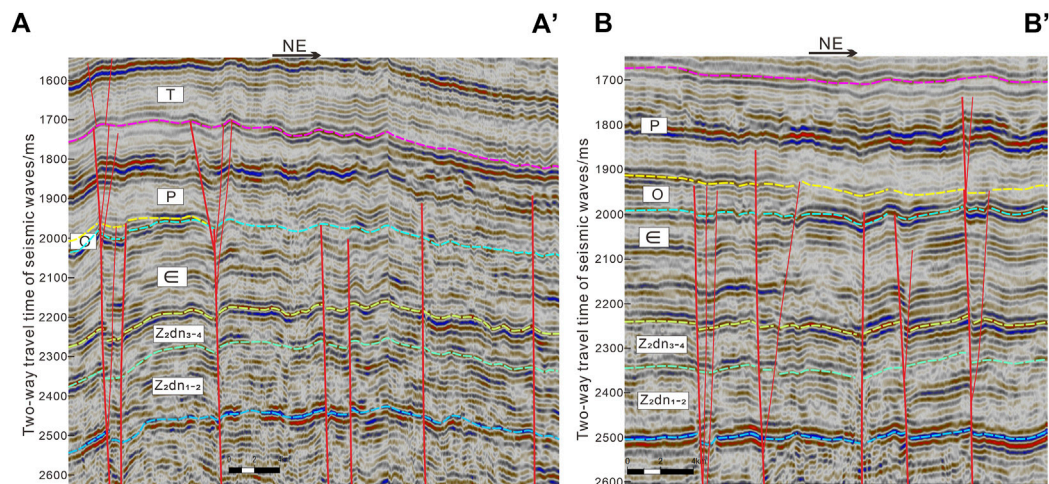


FIGURE 5
Interpreted 3D seismic section (A) A' and (B) B' showing the strike-slip faults. See [Figure 1B](#) for locations.

subparallel and overlap in the map view. The overlapping areas of the soft-linked segments lack significant interaction and obvious deformation. The hard-linked zone shows complex fault networks, with a more complicated overlapping area in the seismic profile ([Figures 6B, 7B, C](#)), suggesting stronger interaction and deformation in the overlap zones. Based on the coherent attribute map extracted from the seismic data that was processed by spectrum decomposition and filtering, different parts of the strike-slip faults in the study area have different structural and planar configuration styles, showing obvious segmentation. To reveal the segmentation characteristics of the strike-slip faults in the study area, the north-west trending fault F3, and north-east trending fault F4 are described and analyzed in this study.

Strike-slip fault F3 is located in the northern part of the study area ([Figure 1C](#)) and extends in a north-west direction. The seismic profile displayed in [Figure 6](#) represents a typical image of F3, which is composed of multiple segments overlapping each other by different fault types to reveal different segmentation along the fault strike. [Figure 6B](#) shows the hard-linked zone, and the main fault is characterized by bifurcation and intertwining from the braided structure section in the plane, exhibiting a transtensional fault with a negative flower structure in the profile. The translational section is a linear extension in the plane, and a highly steep erect fault in the profile, showing few secondary splays, with smaller vertical fault displacements and transtensional features ([Figure 6C](#)). [Figure 6D](#) shows an overlapping zone with right-lateral and right-stepping arrangements in the plane. The interior part of the overlapping zone is in a stretching state, as revealed by the descending block or semi-flower structure in the profile.

The strike-slip fault F4 is a north-east trending fault located in the eastern part of the study area ([Figure 1C](#)), and the main fault shows different segmentation characteristics along the fault strike from south to north ([Figure 7A](#)). [Figure 7B](#) shows the hard-linked zone, segments connecting with each other in the plane, and secondary splays developed in a complicated manner in the overlapping zone, complicating the fault network, while several branch faults

converge and merge into a surface in the profile, forming a positive flower structure. Similar to [Figures 7B, C](#), the hard-linked zone segments in which the cut and left laterally displace the north-west trending fault, developed more fractures due to local stress concentration. [Figure 7D](#) shows a steep upright fault with linear extension in the plan, while [Figure 7E](#) shows the tip of the strike-slip fault, consisting of several branch faults and a main fault, the latter showing a horsetail splay structure in the plane and a semi-flower structure in the profile.

4.3 Analysis of strike-slip fault active periods

Several researchers have conducted extensive studies on the timing of these strike-slip faults ([Yin et al., 2013; Li, 2017; Ma et al., 2018; Su et al., 2020](#)); however, their results have been inconclusive. In this study, based on the investigation of the tectonic evolution of the Central Sichuan area, the active periods of strike-slip faults were determined by jointly using the differences in fault structural styles in different strata, and the fault-cut horizon.

The eastern boundary fault of the Mianzhu-Changning rift serves as the most important normal fault that controls the development of the Gaoshiti-Maoxi paleo uplift, and even the Sinian-Early Cambrian tectonic framework of the entire basin. From the Late Sinian to Early Cambrian, during the Tongwan movement and Xingkai taphrogenesis, strike-slip faults were initially formed in the study area. Due to the uplift and erosion of the Leshan Longnüsi Paleo-uplift that developed in the Early Paleozoic, the Ordovician-Carboniferous was missing in the central Sichuan Basin. Drilling revealed that the Ordovician in the study area was overlapped from southeast to northwest, which was retained only in the Gaoshiti structure area, and missing in the Moxi structure area ([Figures 2, 5](#)). As first-order faults, the southern boundary fault F1 of the Moxi structure, and the northern boundary fault F2 of the Gaoshiti structure had similar structural characteristics in the seismic profile, showing three periods of activity ([Figure 2](#)). The fault cuts through the Sinian

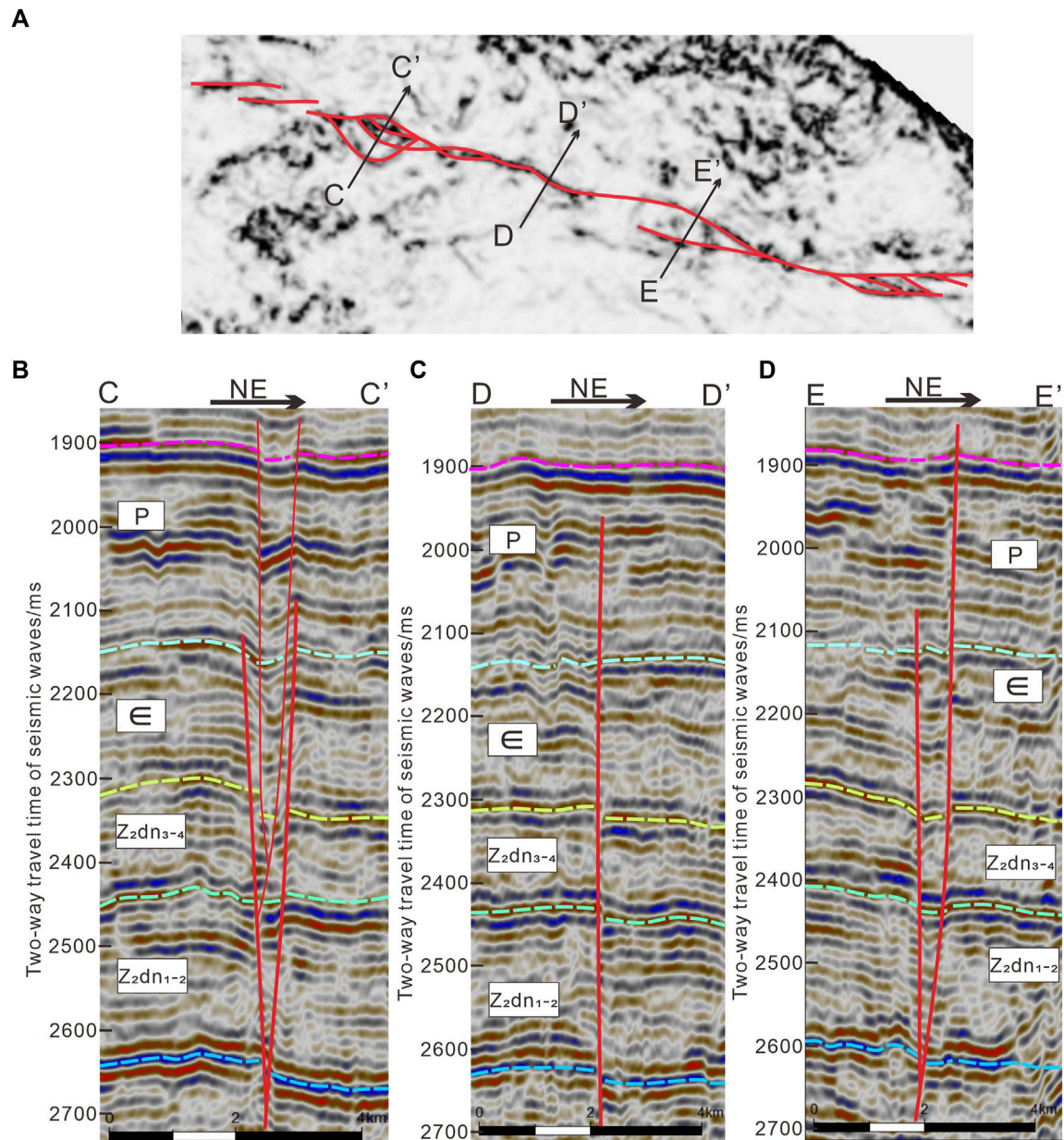


FIGURE 6

(A) The coherence horizon slice of the top of the Sinian, showing segmentation characteristics of the strike-slip fault F3. See Figure 1B for location. (B–D) are interpreted seismic sections of the strike-slip fault F3 from west to east. The location of the seismic sections is shown in Figure 6A.

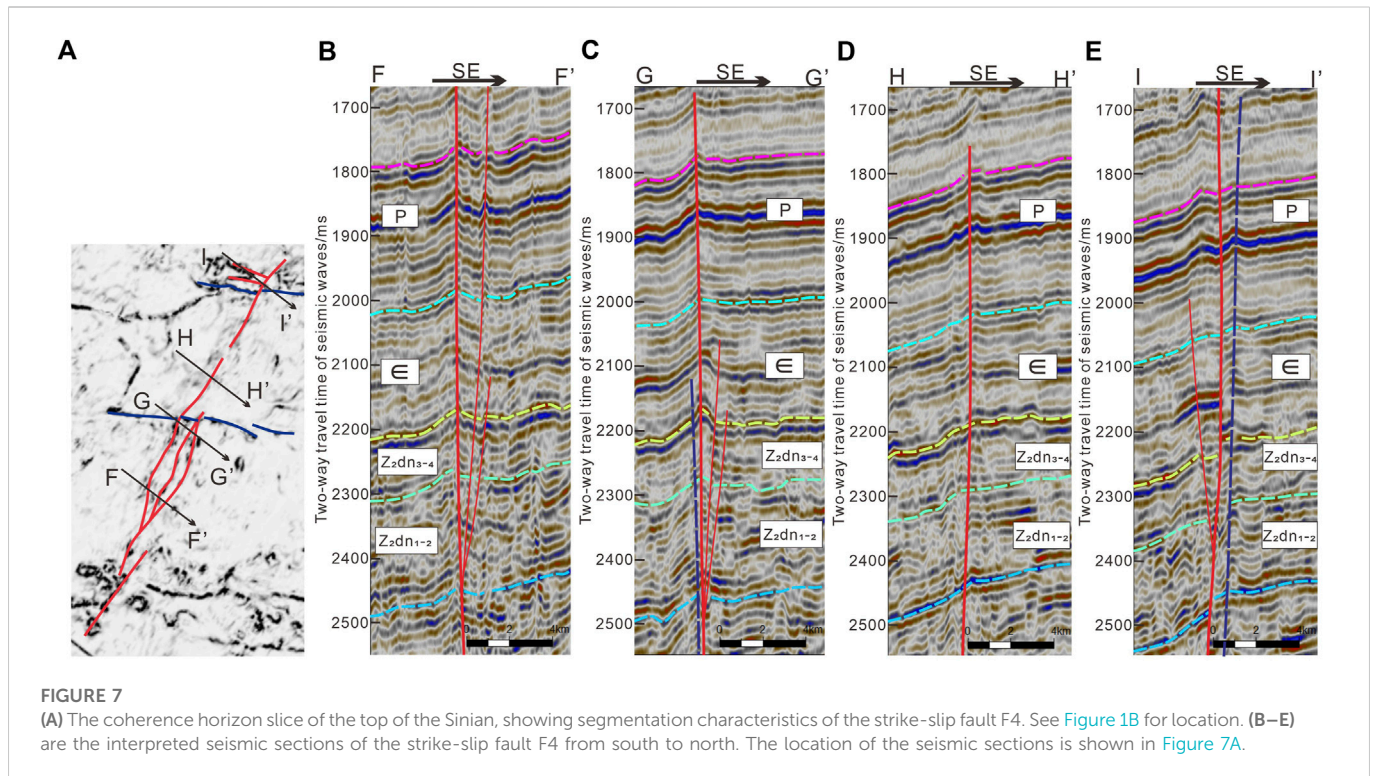
to Lower Triassic strata from bottom to top, while appearing as a highly steep upright strike-slip structure in the Dengying Formation and diverging upward in the Cambrian and Ordovician into a positive flower-like structure. This structure of the Permian was superimposed on the Ordovician, and two flower-like structures were formed. Accordingly, it can be inferred that the strike-slip faults have experienced two fault activities during the deposition of the Ordovician and Permian. The faults formed during the process of fold deformation appear to be perpendicular to the strata (Su et al., 2014a; Su et al., 2014b); therefore, it is speculated that the small horst of the reverse faults perpendicular to the strata in the Triassic may be related to the activities of the Indosinian-Himalayan period subjected to

compressional stresses around the basin, which was the third stage of the strike-slip fault.

5 Discussion

5.1 Superimposed, transformed, reservoir beds

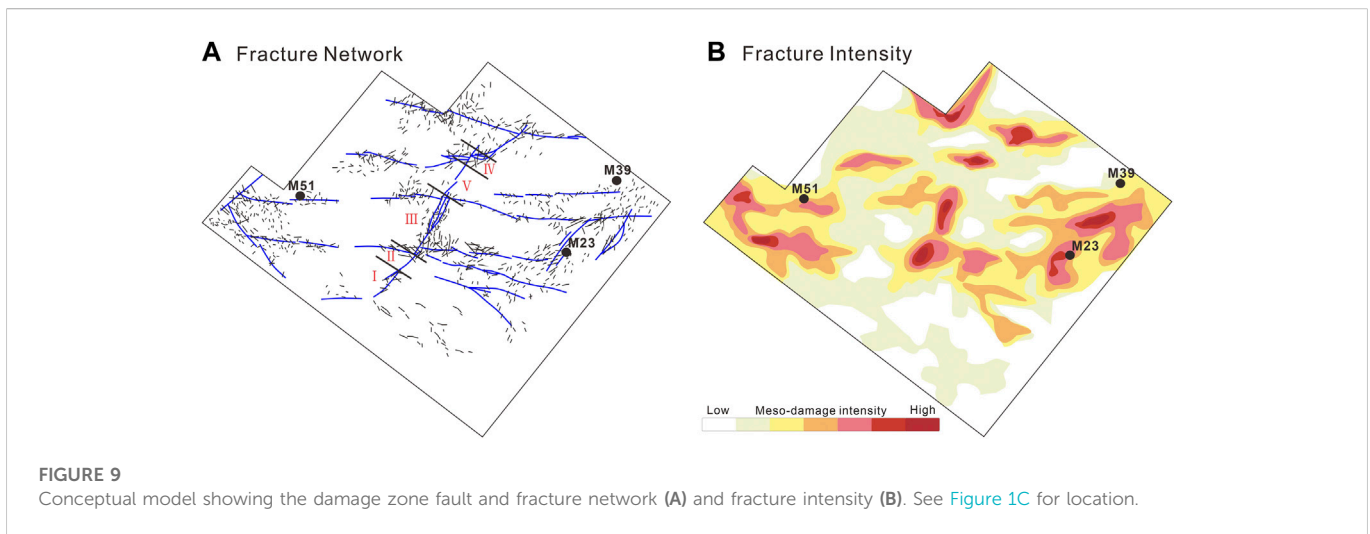
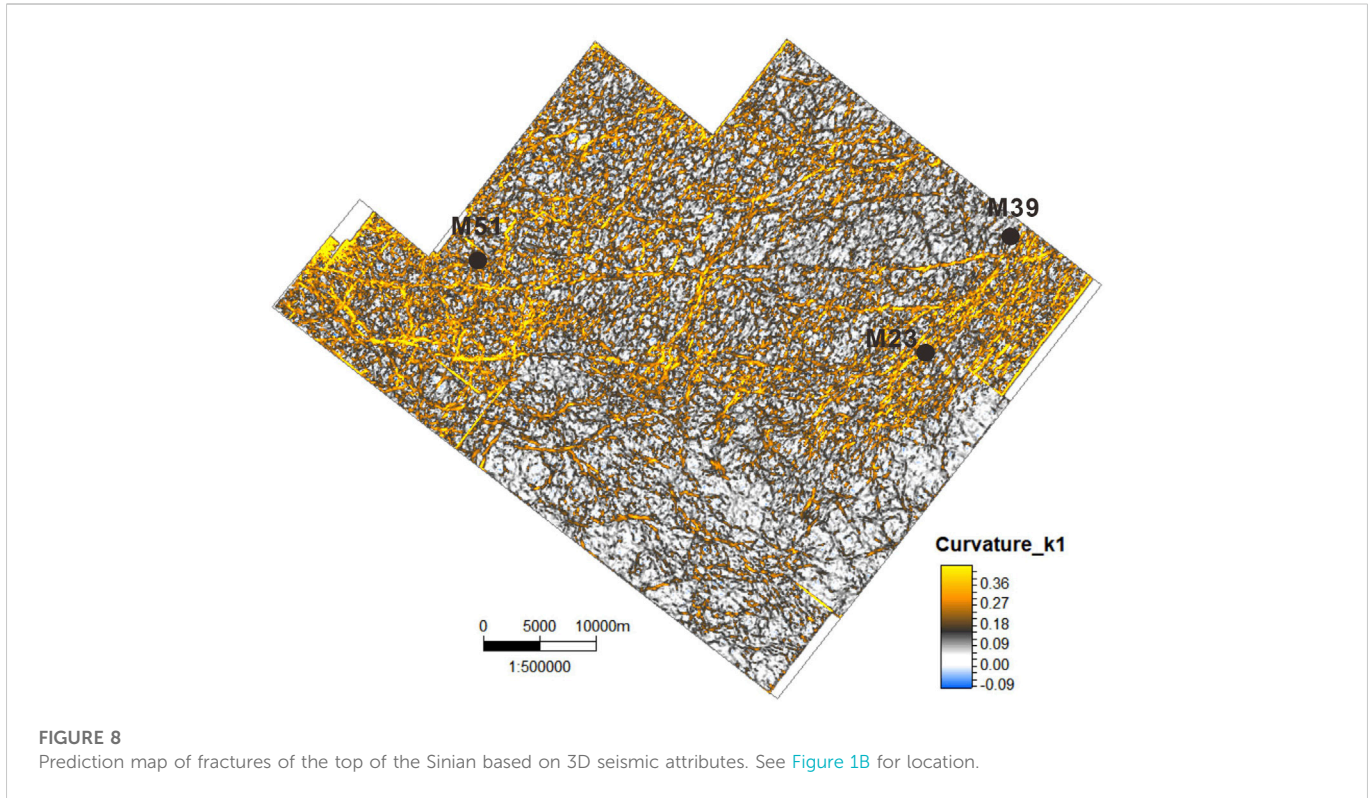
Previous studies have considered that, influenced by diagenetic compaction and cementation, the porosity in carbonate rocks gradually decreases with increasing burial depth. It is difficult to form effective reservoirs in ultradeep formations larger than



6,000 m (Schmoker and Hally, 1982; Ehrenberg et al., 2010; Ehrenberg et al., 2009); however, since the 1990s, China has discovered several deep or ultra-deep large-scale carbonate reservoirs in the Tarim and Sichuan Basins, which have often later undergone significant transformations. Therefore, fault activity and the associated fracture development are particularly important for the formation of high-quality ancient carbonate reservoirs. For example, the fracture-void karst reservoir is developed in the Sinian Dengying Formation of the Sichuan Central Region, and multi-phase fault activities have a strong impact on the late modification of the reservoir, promoting the formation of fractures and increasing the storage space of the reservoir.

Prior research has shown that fractures are composed of both fault cores and fault damage zones (Caine et al., 1996; Aydin, 2000; Kim et al., 2004; Childs et al., 2009; Faulkner et al., 2010; Matonti et al., 2012; Choi et al., 2016; Ostermeijer et al., 2022; Kim et al., 2000). Specifically, fault-damage zones develop branching faults and fractures, while their corresponding degree of development and width are influenced by various factors, such as fault size, stratigraphic lithology, and diagenesis (Tondi, 2007; Agosta et al., 2012; Rotevatn and Bastesen, 2012; Michie, 2015; De Graaf et al., 2017). Typically, the greater the distance from the fault core, the less is the fracture development (Mitchell and Faulkner, 2009; Faulkner et al., 2010; Torabi and Berg, 2011; Johri et al., 2014a). For deep carbonate formations, fault-associated damage zones can effectively improve reservoir performance. Indeed, previous researchers have studied fracture frequency and fault damage zone boundaries at three scales of fracture systems—macro-, medium-, and micro-fractures—based on logs, cores, and thin sections (Wu et al., 2019; Shi et al., 2022). Numerical simulation models with reservoir fracture parameters

have been used to calculate the influence range of major faults that can reach 600–2000 m, and the fracture within the influenced zone is characterized by high density (Xu et al., 2019). The prediction map of fractures based on 3D seismic attributes in the eastern part of the study area reveals the relationship between the distribution characteristics of the fault damage zone and major faults (Figures 8, 9). There are well-developed fractures closer to the major faults owing to stronger tectonic deformation. Many strike-slip faults are composed of multiple segments overlapping each other by different fault types to show different segmentation along the fault strike. The degree of fracture development in different segment types varies according to differential structural style and stress state. On the plot in Figure 10, fault F4 can be divided into five segments horizontally, with the highest throw values, and highest seismic attribute values, reflecting that fractures occur in the hard-linked zone. This suggests that the higher fault throws absorb far more deformation and strain, promoting development of micro-cracks and fractures which are crucial for reservoir transformation. The southern segment I of fault F4 includes soft-linked segments with various displacements. Because they offset the north-west trending faults, the intersection shows significant displacement and greater fracture development. Segments II and IV are linear extensions of the fault plane with less displacement. Secondary splays and fractures in the translational section of the strike-slip fault are less developed, as the structural deformation is mainly concentrated in the main faults, indicating that the surrounding fault damage zones and fractures are limited in development. Segment III shows a braided structure of intersecting transpressional and transtensional faults, maintaining high fracture density, which are the most developed fault damage zones. The northern segment V has mainly



transpressional faults which offset the north-west trending faults, displaying great displacement. The intersection between north-east and north-west faults in the study area shows strong fault activity, producing a wider range of influence, and developing more branch faults and fractures. Faults and their associated fractures serve as high-speed channels for fluid migration, increasing the permeability of reservoirs and enhancing the fluid flow. During the Late Neoproterozoic to Early Cambrian, the faults were active and broke through the surface, providing channels for atmospheric fresh water to flow downward along the fractures. Simultaneously, atmospheric fresh water caused

dissolution of the rocks surrounding the fractures and cracks, forming a 3D fracture-void network. The secondary pores in the reservoir are often too scattered to form an effective interconnection; therefore, unfilled or partially filled fractures can create an interconnected network for isolated pores and form a fracture-pore system at a certain scale, thereby increasing reservoir permeability (Figure 11). The reservoir exhibits low frequency, medium amplitude, and medium continuity reflection characteristics on the seismic profile (Figure 12). The 3D seismic attributes were used to describe the planar distribution of the carbonate reservoir of the Fourth Member Dengying Formation in the eastern part of the study area (Figure 13). It was found that the

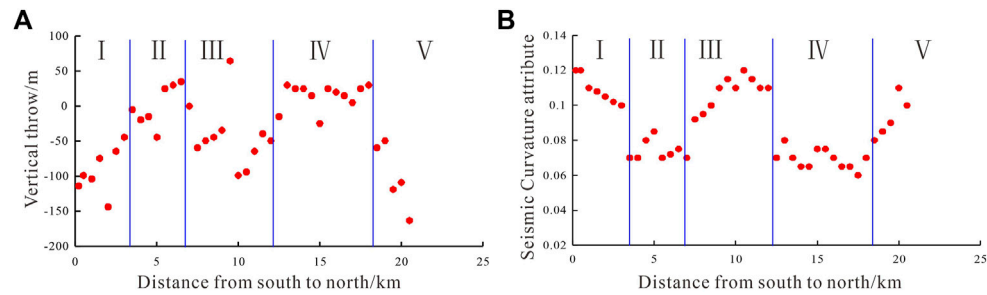


FIGURE 10 (A) The fault segmentation and variations of fault throw along strike-slip fault F4. (B) Distance versus Seismic attribute reflecting fractures (see the fault location in Figures 1C, 9A).

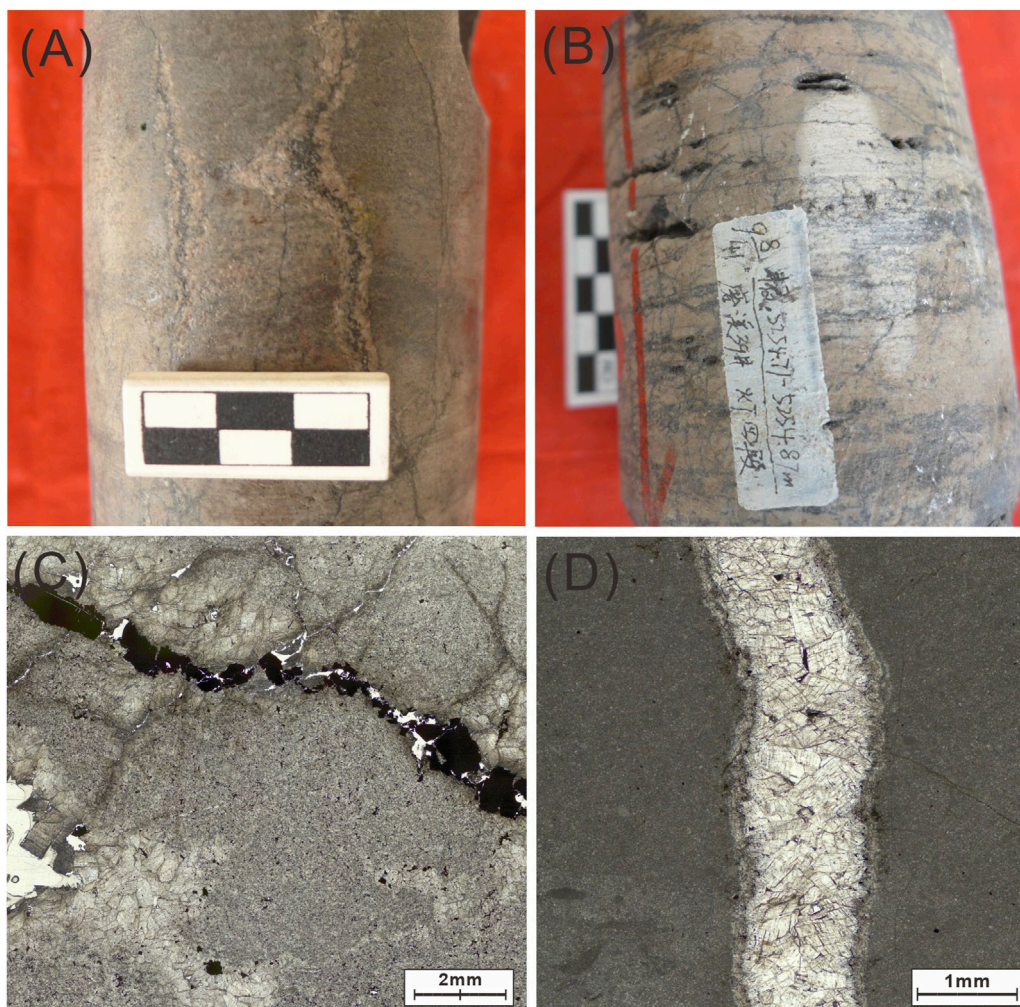
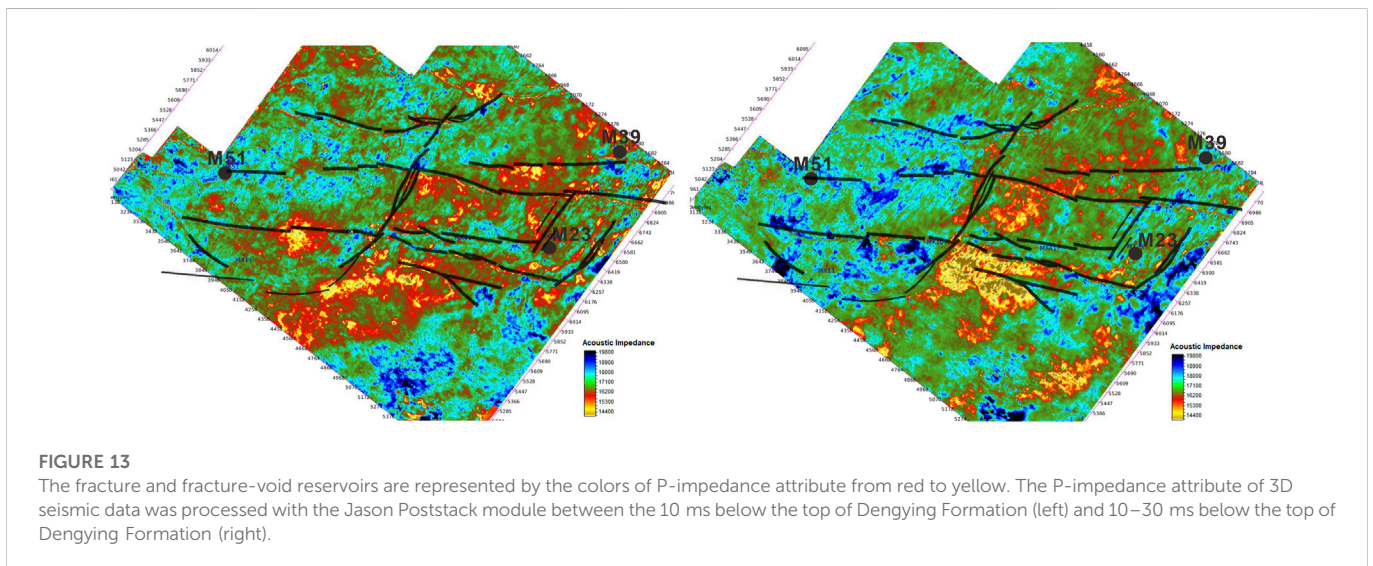
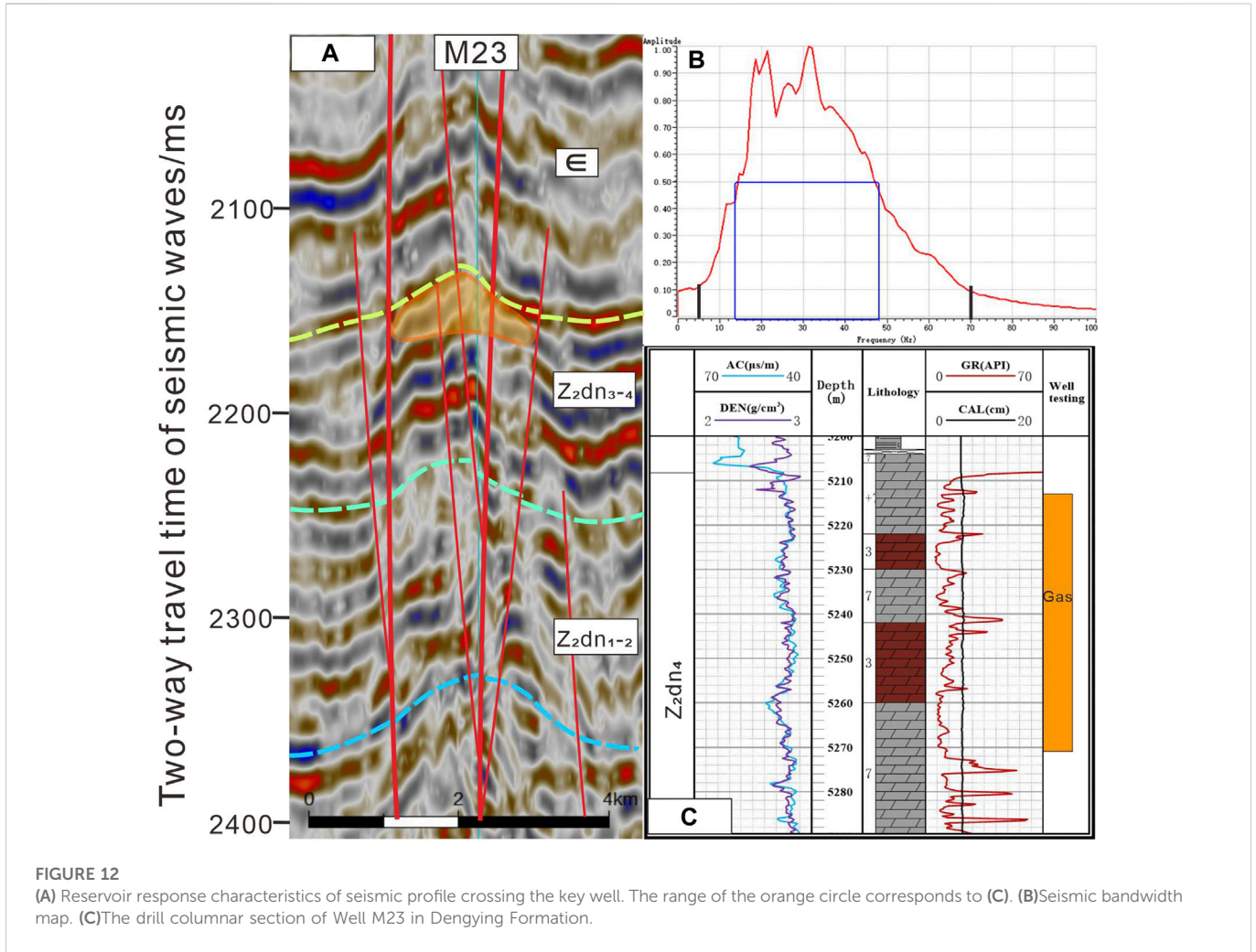


FIGURE 11 Typical photos showing the fractured rocks from the cores (A, B) and thin sections (C, D) in the Dengying reservoir in Central Sichuan Basin. (A) High angle dissolved fracture in clotted dolomite, filled with the saddle dolomite and bitumen, Well M51, 5358.83 m; (B) Reticulated structural fractures with dissolution cavities developed. Well M39, 5254.71 m; (C) Partially filled structural fractures connecting intergranular pores, Well G20, 5184.4 m, plane polarized light; (D) Saddle dolomite vein filling along the fractures, Well M105, 5329.5 m, plane polarized light.

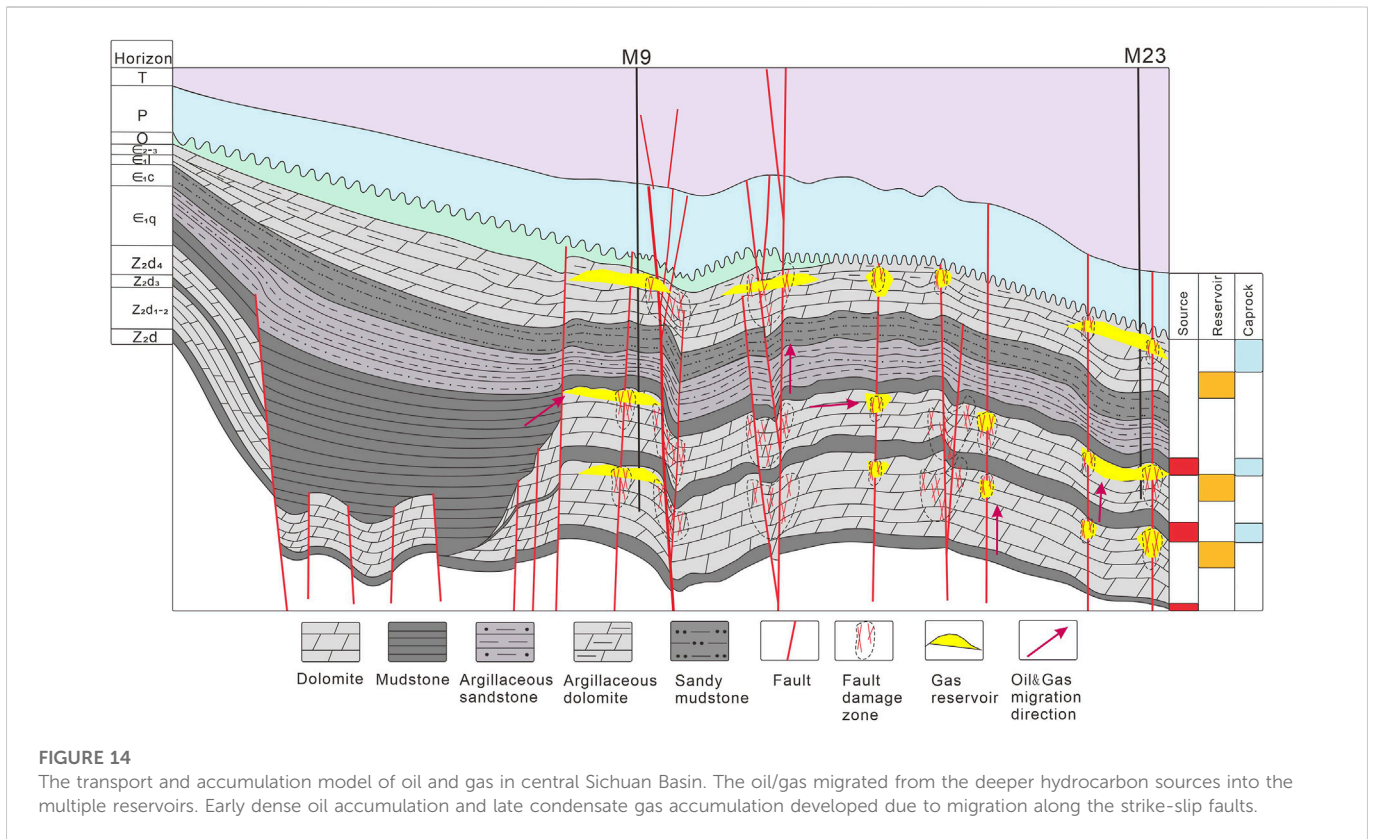
reservoir is mainly distributed along the strike-slip fault. The closer the main fault was, the more fractures developed, providing more channels for fluid migration. Differential segmentation of the strike-

slip fault is associated with varying reservoir quality. The hard-linked zone, such as the braided structure section, formed by bifurcation and interweaving of branch faults where fractures are developed, is



conductive to the development of high-quality reservoirs. Such development is attributed to faults and fractures serving as downwelling channels for shallow groundwater, and upwelling channels for deep hydrothermal fluids, which increases the contact area between the fluids and the original rock, thus

creating favorable conditions for the development of karst reservoirs. The soft-linked segments include few secondary splays, forming moderate quality reservoirs. Compared to other sections, few fractures developed in the translational sections of the strike-slip fault, suggesting poor reservoir quality.



5.2 Hydrocarbon migration pathway

The Sichuan Basin has deposited huge amounts of sedimentary rock since the Sinian and has developed several hydrocarbon source rocks and source-reservoir-cap rock assemblages. Research has shown that the three main hydrocarbon source rocks are the Cambrian Qiongzhusi Formation mudstone, Silurian Longmaxi Formation mudstone, and coal-bearing mudstone of the Xujiache Formation, as well as others, such as the mudstone of the Shisantuo Formation, Lower Permian mudstone, Upper Permian mudstone, and Lower Jurassic mudstone. There are many hydrocarbon-bearing formations, covering almost all formations from the Sinian to the Jurassic. The Sinian source-reservoir-cap rock assemblages are the first, and the oldest marine formation source-reservoir-cap rock combinations in the central Sichuan area, with mudstone of the Doushantuo Formation, the Third member Dengying Formation, and the Cambrian Qiongzhusi Formation mudstone comprising the main hydrocarbon source rocks, algal dolomite of the Second member and Fourth member Dengying Formations serving as the reservoirs, and the Lower Cambrian mudstone as the main cap rock, containing three types of combinations: Upper-Source and Lower-Reservoir, Upper-Source and Lateral- Reservoir, and Lower-Source and Upper-Reservoir (Figure 14).

Based on the seismic interpretation results of the whole study area, and oil and gas shows from the exploration, the development of high-quality dolomite reservoirs and fault activity in the central area of the Sichuan Basin determines hydrocarbon migration and accumulation (Figure 14), whereas the development of faults and prolonged active periods are conducive to communicating with the effective source rock, serving as favorable conditions for the

production of oil and gas pathways. When source rocks start to produce hydrocarbons, the reservoir of the Sinian Dengying Formation already has storage space, which provides favorable conditions for the formation of paleo-oil reservoirs and crude oil cracking *in situ*. Many studies have been conducted on the oil and gas charging time, as well as the hydrocarbon accumulation period of the Sinian Dengying Formation in the central area of the Sichuan Basin (Liu et al., 2009; Luo et al., 2015; Wang et al., 2016; Shen et al., 2021), and concluded that there were three periods of hydrocarbon accumulation: The first peak period of oil accumulation occurred at the end of the Silurian, but the hydrocarbon supply from source rocks was a continuous process that could have advanced to the early-middle Ordovician at the earliest. This may be the main reason why various scholars considered oil accumulation to have occurred during the Ordovician-Silurian, when a series of strike-slip faults formed with inherited activities in the Late Sinian-Early Cambrian across the central area of the Sichuan Basin. The Wuyi-Yunkai orogeny in the whole Yangtze region occurred due to regional extensional stress, thereby developing secondary splays, and fault damage zones around the main strike-slip faults. Simultaneously, the uplifting stratum suffered significant weathering and denudation, resulting in a wide range of reservoirs being created, with large-scale oil charging. In the late Permian-Early Triassic, the uplift and denudation of formations caused by the rise of the Emeishan mantle plume and the massive eruption of basalts reactivated the faults. The hydrothermal event related to the eruption of the Emeishan basalts caused a large amount of thermal fluid upwelling along these faults and fractures, leading to dissolved carbonate reservoirs, and improved reservoir performance. With the maturation and

charging of hydrocarbons, peak oil accumulation occurred during the second stage. During the Yanshan–Xishan epoch, the crude oil in the Sinian Dengying Formation cracked into gas at great depths and high temperatures, creating the peak period of natural gas accumulation.

6 Conclusion

- (1) Based on 2D and 3D seismic data in the central area of the Sichuan Basin, systematic interpretation of the deep fracture system suggests that steeply dipping faults and flower-like structures were mainly developed in the study area. The three groups of north-west, north-east, and nearly west-east striking faults in the study area exhibit differences in the structural patterns of the southern and northern regions. The planar combination styles of strike-slip faults consist of an en-echelon arrangement, oblique intersection, and arc shape. The slip faults are classified into three levels according to their activity duration, structural deformation degree, and extension length. Owing to the differences between the upper and lower structural styles of the fault system, location of the fault cut-through layer, and deformation characteristics of the strata, the active stage of strike-slip faults is considered to have occurred in four phases: Late Archean–Early Cambrian, Ordovician, Permian, and Triassic. Generally, a strike-slip fault consists of several segments with different dipping and fault throws, leading to planar structural characteristics that change along the fault strike. The interior of the strike-slip fault is composed of linear translational, overlapping, and braided segments. The translational section is a linear extension of the fault plane with a steep upright fault profile. The overlapping section includes an extensional or contractional segment controlled by its rotational direction relative to the step, whereas the braided section contains interlocking transtensional or transpressional structural segments.
- (2) The control of strike-slip faults on fracture development in the study area is significant, including the control of main faults on secondary splays and fracture development. The degree of intensity and period of fault activity impacts the development of the surrounding fracture zones, with a greater distance from the fault resulting in lower density and intensity of fracture. Segmentation of strike-slip faults governs the distribution of karst reservoirs in the Sinian Dengying Formation. The most developed reservoirs are in the overlapping and braided sections, and relatively undeveloped reservoirs are in the linear translational sections.
- (3) Deep strike-slip faults have great significance for oil and gas exploration in the central Sichuan Basin. Small fault and fracture systems induced by major fault activities can form interconnections for isolated pores, effectively improving reservoir properties, and increasing oil and gas production. Deep fault activities cause tectonic deformation of the surrounding rock, which can control the formation of traps.

These serve as favorable channels for oil and gas migration, effectively communicating with hydrocarbon source rocks and reservoirs, and resulting in the formation of oil and gas reservoirs.

Data availability statement

The original contributions presented in the study are included in the article/supplementary material, further inquiries can be directed to the corresponding author.

Ethics statement

Ethical review and approval was not required for the study on human participants in accordance with the local legislation and institutional requirements. Written informed consent for participation was not required for this study in accordance with the national legislation and the institutional requirements.

Author contributions

SL collected and processed the data, plotted the figures used in this study, and wrote the manuscript. ZL guided this work. WZ provided helpful discussions and suggestions. YG offered constructive comments. All authors contributed to the article and approved the submitted version.

Funding

This research was funded by the Strategic Priority Research Program of the Chinese Academy of Sciences (Grant No. XDA14010201).

Conflict of interest

The authors declare that the research was conducted in the absence of any commercial or financial relationships that could be construed as a potential conflict of interest.

Publisher's note

All claims expressed in this article are solely those of the authors and do not necessarily represent those of their affiliated organizations, or those of the publisher, the editors and the reviewers. Any product that may be evaluated in this article, or claim that may be made by its manufacturer, is not guaranteed or endorsed by the publisher.

References

Agosta, F., Ruano, P., Rustichelli, A., Tondi, E., Galindo-Zaldívar, J., and Sanz de Galdeano, C. (2012). Inner structure and deformation mechanisms of normal faults in

conglomerates and carbonate grainstones (Granada Basin, Betic Cordillera, Spain): Inferences on fault permeability. *J. Struct. Geol.* 45, 4–20551. doi:10.1016/j.jsg.2012.04.003

- An, S., Chen, Y., Luo, M., and Yan, S. (2021). Three dimensional fault enhancement technique based on multidirectional recognition. *Acta Sci. Nat. Univ. Pekin.* 57, 653–659.
- Aydin, A. (2000). Fractures, faults and hydrocarbon entrapment, migration and flow. *Mar. Pet. Geol.* 17, 797–814. doi:10.1016/S0264-8172(00)00020-9
- Aydin, A., and Berryman, J. G. (2010). Analysis of the growth of strike-slip faults using effective medium theory. *J. Struct. Geol.* 32, 1629–1642. doi:10.1016/j.jsg.2009.11.007
- Caine, J. S., Evans, J. P., and Forster, C. B. (1996). Fault zone architecture and permeability structure. *Geol.* 24, 1025–1028. doi:10.1130/0091-7613(1996)024<1025:fzaaps>2.3.co;2
- Chen, Q., Sun, M., Long, X., Zhao, G., Wang, J., Yu, Y., et al. (2018). Provenance study for the Paleozoic sedimentary rocks from the west Yangtze Block: Constraint on possible link of South China to the Gondwana supercontinent reconstruction. *Precambrian Res.* 309, 271–289. doi:10.1016/j.precamres.2017.01.022
- Childs, C., Manzocchi, T., Walsh, J. J., Bonson, C. G., Nicol, A., and Schöpfer, M. P. J. (2009). A geometric model of fault zone and fault rock thickness variations. *J. Struct. Geol.* 31, 117–127. doi:10.1016/j.jsg.2008.08.009
- Choi, J. H., Edwards, P., Ko, K., and Kim, Y. S. (2016). Definition and classification of fault damage zones: A review and a new methodological approach. *Earth-Science Rev.* 152, 70–87. doi:10.1016/j.earscirev.2015.11.006
- Chopra, S., and Marfurt, K. J. (2007). *Seismic attributes for prospect identification and reservoir characterization*[R]. Tulsa: Society of Exploration Geophysicists.
- Ehrenberg, S. N., Nadeau, P. H., and Steen, Ø. (2009). Petroleum reservoir porosity versus depth: Influence of geological age. *Bulletin* 93, 1281–1296. doi:10.1306/06120908163
- Ehrenberg, J. H. (2010). *Oil and gas exploration of cambrian-ordovician carbonate in Tarim Basin*. Beijing: Petroleum Industry Press.
- Faulkner, D. R., Jackson, C. A. L., Lunn, R. J., Schlische, R. W., Shipton, Z. K., Wibberley, C. A. J., et al. (2010). A review of recent developments concerning the structure, mechanics and fluid flow properties of fault zones. *J. Struct. Geol.* 32, 1557–1575. doi:10.1016/j.jsg.2010.06.009
- Feng, Y., Wen, Z., Zheng, Q., Mao, X., Hou, F., Qi, J., et al. (2011). A review of progress in paleocontinent reconstruction research in China. *Mar. Geol. Front.* Available at: <http://www.jhyyq.com.cn/en/article/id/f7e86fbd-0297-47a3-96ce-3f72bfd32fb8> 27, 41–49.
- Gu, Z., and Wang, Z. (2014). The discovery of neoproterozoic extensional structures and its significance for gas exploration in the central sichuan block, Sichuan Basin, south China. *Sci. China Earth Sci.* 57, 2758–2768. doi:10.1007/s11430-014-4961-x
- He, Z. L., Ma, Y. S., Zhu, D. Y., Duan, T. Z., Geng, J. H., Zhang, J. T., et al. (2021). Theoretical and technological progress and research direction of deep and ultra-deep carbonate reservoirs. *Oil Gas. Geol.* 42, 533–546. doi:10.11743/ogg20210301
- Hou, F., Zhang, X., Feng, Y., Sun, J., Wen, Z., Gao, Z., et al. (2014). Paleogeographic reconstruction and tectonic evolution of major blocks in China since Paleozoic. *Mar. Geol. Quatern. Geol.* 34, 9–26. doi:10.3724/SP.J.1140.2014.06009
- Hu, F., Liu, S., Santosh, M., Deng, Z., Wang, W., Zhang, W., et al. (2015). Chronology and tectonic implications of neoproterozoic blocks in the South qinling orogenic belt, central China. *Gondwana Res.* 30, 24–47. doi:10.1016/j.gr.2015.01.006
- Jiang, G. Q., Shi, X. Y., Zhang, S. H., Wang, Y., and Xiao, S. (2011). Stratigraphy and paleogeography of the ediacaran Doushantuo Formation (ca. 635–551Ma) in south China. *Gondwana Res.* 19, 831–849. doi:10.1016/j.gr.2011.01.006
- Johri, M., Dunham, E. M., Zoback, M. D., and Fang, Z. (2014a). Predicting fault damage zones by modeling dynamic rupture propagation and comparison with field observations. *J. Geophys. Res. Solid Earth* 119, 1251–1272. doi:10.1002/2013JB010335
- Khalil, S. M., and McClay, K. R. (2016). 3D geometry and kinematic evolution of extensional fault-related folds, NW Red Sea, Egypt. *Geol. Soc. Lond. Spec. Publ.* 439, 11. doi:10.1144/sp439.11
- Kim, Y. S., Andrews, J. R., and Sanderson, D. J. (2000). Damage zones around strike-slip fault systems and strike-slip fault evolution, Crackington Haven, southwest England. *Geosci. J.* 4, 53–72. doi:10.1007/bf02910127
- Kim, Y. S., Peacock, D. C. P., and Sanderson, D. J. (2004). Fault damage zones. *J. Struct. Geol.* 26, 503–517. doi:10.1016/j.jsg.2003.08.002
- Kim, Y. S., and Sanderson, D. J. (2005). The relationship between displacement and length of faults: A review. *Earth-Science Rev.* 68, 317–334. doi:10.1016/j.earscirev.2004.06.003
- Li, S. (2017). Study on fault characteristics in moxi-gaoshiti area, Sichuan Basin. [Master's thesis]. East China: CUPB.
- Li, Y., Xue, Z., Cheng, Z., and Jiang, H. (2020). Progress and development directions of deep oil and gas exploration and development in China. *China Pet. explor.* 25, 46–57. doi:10.3969/j.issn.1672-7703.2020.01.005
- Li, Z., Ran, B., Xiao, B., and Song, J. (2019). Sinian-Early Cambrian uplift-depression pattern in the northern margin of Sichuan Basin and its significance for oil and gas exploration. *Earth Sci. Front.* 26, 59–85.
- Liang, S., and Li, Z. (2022). Development characteristics and formation mechanism of deep strike-slip faults in Central Sichuan basin based on seismic data interpretation. *Fresenius Environ. Bull.* Available at: https://www.prt-parlar.de/download_feb_2022/ 31 (06), 6230–6240.
- Liu, S., Ma, Y., Cai, X., Xu, G., Wang, G., Yong, Z., et al. (2009). Characteristic and accumulation process of the natural gas from sinian to lower paleozoic in Sichuan Basin, China. *J. Chengdu Univ. Technol. Sci. Technol. Ed.* 36, 345–354.
- Liu, W., Meng, Q., Zhang, G., and Zhang, L. (2010). Geologic characteristics of oil and gas reservoir in old Lower Paleozoic and Sinian carbonate rocks. *Mar. Orig. Pet. Geol.* 15, 15–20.
- Liu, S., Sun, W., Luo, Z., and Song, J. (2013). Xingkai geo-fissure movement and oil and gas exploration of lower assemblage in Sichuan Basin. *Chengdu Univ. Technol. Chin. J. Sci. Nat. Sci. Ed.* 40, 511–520. doi:10.1016/s1876-3804(13)60057-9
- Luo, B., Luo, W. J., Wang, W., Wang, Z., and Shan, S. (2015). Formation mechanism of the sinian natural gas reservoir in the leshan-longnvisi paleo-uplift, Sichuan Basin. *Nat. Gas. Geosci.* Available at: <http://www.nggs.ac.cn/EN/10.11764/j.issn.1672-1926.2015.03.0444> 26, 444–455.
- Luo, Z., Liu, S., Liu, S., Yong, Z., Zhao, X., and Sun, W. (2004). The action of “Emei mantle plume” on the separation of the Yangtze plate from the Tarim plate and its significance in exploration. *Acta Geosci. Sin.* 25, 515–522.
- Ma, D., Wang, Z., Duan, S., Gao, J., Jiang, Q., Jiang, H., et al. (2018). Strike-slip faults and their significance for hydrocarbon accumulation in Gaoshiti-Moxi area, Sichuan Basin, SW China. *Petroleum Explor. Dev.* 45, 851–861. doi:10.1016/S1876-3804(18)30088-0
- Ma, Y., Li, H., Liu, K., Gu, H., and Ren, H. (2020). Application of ant tracking technology based on frequency division coherence in fault characterization of Tare Oilfield. *Geophys. Prospect. Pet.* 59, 258–266. doi:10.3969/j.issn.1000-1441.2020.02.012
- Matonti, C., Lamarche, J., Guglielmi, Y., and Marić, L. (2012). Structural and petrophysical characterization of mixed conduit/seal fault zones in carbonates: Example from the Castellans fault (SE France). *J. Struct. Geol.* 39, 103–121. doi:10.1016/j.jsg.2012.03.003
- Michie, E. A. H. (2015). Influence of host lithofacies on fault rock variation in carbonate fault zones: A case study from the island of Malta. *J. Struct. Geol.* 76, 61–79. doi:10.1016/j.jsg.2015.04.005
- Mitchell, T. M., and Faulkner, D. R. (2009). The nature and origin of off-fault damage surrounding strike-slip fault zones with a wide range of displacements: A field study from the atacama fault system, northern Chile. *J. Struct. Geol.* 31, 802–816. doi:10.1016/j.jsg.2009.05.002
- Moghadam, H. S., Khademi, M., Hu, Z., Stern, R. J., Santos, J. F., and Wu, Y. (2013). Cadomian (Ediacaran-Cambrian) arc magmatism in the ChahJam- Biarjmand metamorphic complex (Iran): Magmatism along the northern active margin of Gondwana. *Gondwana Res.* 27, 439–452. doi:10.1016/j.gr.2013.10.014
- Nemcok, M., Schamel, S., and Gayer, R. (2005). *Thrustbelts: Structural architecture, thermal regimes and petroleum systems*. New York: Cambridge University Press.
- Niu, Y., O'Hara, M. J., and Pearce, J. A. (2003). Initiation of subduction zones as a consequence of lateral compositional buoyancy contrast within the lithosphere: A petrological perspective. *J. Pet.* 44, 851–866. doi:10.1093/petrology/44.5.851
- Ostermeijer, G. A., Aben, F. M., Mitchell, T. M., Rockwell, T. K., Rempe, M., and Farrington, K. (2022). Evolution of co-seismic off-fault damage towards pulverisation. *Earth Planet. Sci. Lett.* 579, 117353. doi:10.1016/j.epsl.2021.117353
- Rotevatn, A., and Bastesen, E. (2012). Fault linkage and damage zone architecture in tight carbonate rocks in the suz rift (Egypt): Implications for permeability structure along segmented normal faults. *Sp* 374, 79–95. doi:10.1144/sp374.12
- Schmokler, J. W., and Hally, R. B. (1982). Carbonate porosity versus depth: A predictable relation for south Florida. *AAPG Bull.* 66, 2561–2570.
- Shen, A., Zhao, W., Hu, A., Wang, H., Feng, L., and Wang, Y. (2021). The dating and temperature measurement technologies for carbonate minerals and their application in hydrocarbon accumulation research in the paleo-uplift in central Sichuan Basin, SW China. *Pet. explor. Dev.* 48, 476–487. doi:10.1016/s1876-3804(21)60045-9
- Shi, J., Zhao, X., Pan, R., Zeng, L., and Luo, W. (2022). Natural fractures in the deep Sinian carbonates of the central Sichuan Basin, China: Implications for reservoir quality. *J. Petroleum Sci. Eng.* 216, 110829. doi:10.1016/j.petrol.2022.110829
- Stein, S., and Stein, C. A. (2013). Thermo-mechanical evolution of oceanic lithosphere: Implications for the subduction process and deep earthquakes. *Wash. D.C. Am. Geophys. Union Geophys. Monogr. Ser.* 96, 1–17. doi:10.1029/gm096p0001
- Su, N., Yang, W., Yuan, B., Dai, X., Wang, X., Wu, S., et al. (2020). Structural features and deformation mechanism of transtensional faults in Himalayan period, Sichuan Basin. *Earth Sci.* 46, 1–7. doi:10.3799/dqkx.2020.202
- Su, N., Zou, L. J., Shen, X., Guo, F., Ren, Y., Xie, Y., et al. (2014b). Fracture patterns in successive folding in the western Sichuan Basin, China. *J. Asian Earth Sci.* 81, 65–76. doi:10.1016/j.jseas.2013.12.003
- Su, N., Zou, L. J., Shen, X., Wu, W., Zhang, G., Kong, F., et al. (2014a). Identification of fracture development period and stress field analysis based on fracture fabrics in tectonic superposition areas. *Arab. J. Geosci.* 7, 3983–3994. doi:10.1007/s12517-013-1063-6
- Tondi, E. (2007). Nucleation, development and petrophysical properties of faults in carbonate grainstones: Evidence from the San Vito Lo Capo peninsula (Sicily, Italy). *J. Struct. Geol.* 29, 614–628. doi:10.1016/j.jsg.2006.11.006
- Tong, H., Cai, D., Wu, Y., Li, X., Li, X., and Meng, L. (2010). Activity criterion of pre-existing fabrics in non-homogeneous deformation domain. *Sci. China Earth Sci.* 53, 1115–1125. doi:10.1007/s11430-010-3080-6
- Torabi, A., and Berg, S. S. (2011). Scaling of fault attributes: A review. *Mar. Petroleum Geol.* 28, 1444–1460. doi:10.1016/j.marpetgeo.2011.04.003

- Wang, R., Xu, Z., Santosh, M., Xu, X., Deng, Q., and Fu, X. (2017). Middle Neoproterozoic (ca. 705–716 Ma) arc to rift transitional magmatism in the northern margin of the Yangtze Block: Constraints from geochemistry, zircon U-Pb geochronology and Hf isotopes. *J. Geodyn.* 109, 59–74. doi:10.1016/j.jog.2017.07.003
- Wang, Z., Wang, T., Wen, L., Jiang, H., and Zhang, B. (2016). Basic geological characteristics and accumulation conditions of Anyue giant gas field, Sichuan Basin. *China Offshore Oil Gas.* 28, 45–52.
- Wei, G., Wang, Y., and Xiao, S. (2019). *Structural characteristics and oil and gas in Sichuan Basin [M]*. Beijing, Science Press.
- Wu, G., Gao, L., Zhang, Y., Ning, C., and Xie, E. (2019). Fracture attributes in reservoir-scale carbonate fault damage zones and implications for damage zone width and growth in the deep subsurface. *J. Struct. Geol.* 118, 181–193. doi:10.1016/j.jsg.2018.10.008
- Xiang, Z., Yan, Q., White, J. D. L., Song, B., and Wang, Z. (2015). Geochemical constraints on the provenance and depositional setting of Neoproterozoic volcanoclastic rocks on the northern margin of the Yangtze Block, China: Implications for the tectonic evolution of the northern margin of the Yangtze Block. *Precambrian Res.* 264, 140–155. doi:10.1016/j.precamres.2015.04.012
- Xu, K., Dai, J., Feng, J., and Ren, Q. (2019). Fault system and its controlling effect on fracture distribution in Moxi-Gaoshiti block, Sichuan Basin, China. *J. Southwest Pet. Univ.* 41, 10–22. doi:10.11885/j.issn.1674-5086.2018.01.10.01
- Yin, J., Gu, Z., and Li, Q. (2013). Characteristics of deep-rooted faults and their geological significances in Dachuanzhong area, Sichuan Basin. *Oil Gas. Geol.* 34, 376–382. doi:10.11743/ogg20130314
- Zeng, H. (2017). RGB blending of frequency panels: A new useful tool for high-resolution 3D stratigraphic imaging. *Interpretation* 5, 1–46. doi:10.1190/segam2017-17494930.1
- Zhang, J., Zhang, H., and Li, L. (2018). Neoproterozoic tectonic transition in the South Qinling Belt: New constraints from geochemistry and zircon U-Pb-Hf isotopes of diorites from the Douling Complex. *Precambrian Res.* 306, 112–128. doi:10.1016/j.precamres.2017.12.043
- Zhu, M., Zhang, J., and Yang, A. (2007). Integrated ediacaran (sinian) chronostratigraphy of south China. *Palaeogeogr. Palaeoclimatol. Palaeoecol.* 254, 7–61. doi:10.1016/j.palaeo.2007.03.025
- Zhu, X., Chen, F., Liu, B., Zhang, H., and Zhai, M. (2015). Geochemistry and zircon ages of mafic dikes in the South Qinling, central China: Evidence for Late Neoproterozoic continental rifting in the northern Yangtze block. *Int. J. Earth Sci. Geol. Rundsch.* 104, 27–44. doi:10.1007/s00531-014-1056-z
- Zhu, X., Chen, F., Nie, H., Siebel, W., Yang, Y., Xue, Y., et al. (2014). Neoproterozoic tectonic evolution of South Qinling, China: Evidence from zircon ages and geochemistry of the Yaolinghe volcanic rocks. *Precambrian Res.* 245, 115–130. doi:10.1016/j.precamres.2014.02.005